A poroelastic model for the tidal modulation of seafloor hydrothermal systems

Tim Jupp

BP Institute for Multiphase Flow, University of Cambridge, Cambridge, U.K.

Adam Schultz[1]

School of Earth, Ocean and Planetary Sciences, Cardiff University, Cardiff, U.K.

Abstract.

Time–series measurements of the temperature and exit velocity of hydothermal effluent suggest that seafloor hydrothermal systems are modulated by tidal processes. Here, we apply the theory of poroelasticity to predict the magnitude and phase of tidally induced changes in the temperature and flow rate of hydrothermal effluent at the seafloor. We construct a model in which the steady–state upwelling of buoyant fluid in the crust is modulated by tidal loading of a one–dimensional seafloor by the overlying water column. The nature of the solution is controlled by the relative magnitudes of three length scales. These are: (1) the depth H of the heat source below the seafloor, (2) the skin depth D over which pore pressure signals can diffuse during one tidal cycle and (3) the advective length scale A over which the upwelling flow advects thermal signals during one tidal cycle. We consider the likely magnitude of the parameters in a real system as well as the limitations of a one–dimensional representation of that system. We then discuss how observational data on the magnitude and phase lag of temperature and flow rate could be used to constrain the sub–seafloor parameters that govern hydrothermal circulation within the seafloor.

1. Introduction

There are many examples of the apparent modulation at tidal periods of the physical, chemical or biological characteristics of seafloor hydrothermal systems [e.g. *Sato et al.*, 1995; *Fujioka et al.*, 1997; *Davis and Becker*, 1994; *Davis et al.*, 1995; *Davis and Becker*, 1999; *Kinoshita et al.*, 1996; *Kinoshita et al.*, 1998; *Schultz et al.*, 1992; *Schultz et al.*, 1996; *Johnson et al.*, 1994; *Chevaldonné et al.* 1991; *Fornari et al.*, 1998; *Little et al.*, 1988; *Little et al.*, 1989; *Wetzler et al.*, 1998; *Rudnicki et al.*, 1994; *Johnson and Tunnicliffe*, 1985; *Kadko*, 1994; *Cooper*, 1999; *Copley et al.*, 1999; *McDuff and Delaney*, 1995; *Delaney et al.*, 1997; *Tolstoy et al.*, 2002]. Variations in the temperature, flow rate and chemical composition of hydrothermal effluent can often be correlated to the local ocean tide, and so it is suspected that the changing tidal pressure field on the seafloor is responsible for these observed tidal signals. The aim of this paper is to establish a simple physical model for the tidal modulation of a hydrothermal system that predicts the magnitude and phase of the temperature and exit velocity of diffuse hydrothermal effluent at the point of emission from the seafloor, relative to the local ocean tide (Figure 1).

We investigate the effect of tidal loading on hydrothermal systems by considering the equations of poroelasticity, which describe the response of a fluid–filled poroelastic medium to applied stress [*Biot*, 1941; *Rice and Cleary*, 1976; *Van der Kamp and Gale*, 1983; *Kümpel*, 1991]. When the medium is placed under load, the resultant stress is borne partly by the solid matrix and partly by the interstitial fluid. In the absence of fluid flow, the partitioning of the stress is controlled by the porosity, the elastic properties of the solid matrix and the bulk modulus of the fluid. The proportion of the total stress that is borne by the fluid is manifest as a change in fluid pressure, which we term the 'incremental pore pressure' $\hat{p}$. If there are any spatial gradients or discontinuities in elastic properties, spatial gradients in the incremental pore pressure are induced, even for a locally uniform load such as the ocean tide. In a permeable medium these pressure gradients drive a flux of interstitial fluid according to Darcy's Law, ensuring that any changes in incremental pore pressure are subject to diffusion when fluid is able to flow.

The most obvious place where there is a sharp discontinuity in elastic properties is the seafloor itself. The tides induce an incremental pore pressure signal that diffuses away from this boundary into the crust [*Van der Kamp and Gale*, 1983]. *Wang and Davis* (1996) have shown that similar diffusive signals are expected at any subseafloor boundaries where the porosity or elastic properties of the solid matrix change. We recognise the existence of such lithological boundaries in a real system and the capacity of such changes in the material properties of the seafloor to influence the hydrology, but our aim here is to consider the influence of the properties of the pore fluid on the hydrological response to tidal pressure loading.

[1]Now at College of Oceanic and Atmospheric Sciences, Oregon State University, Corvallis, OR, U.S.A.

Paper number .
0148-0227/04/$9.00

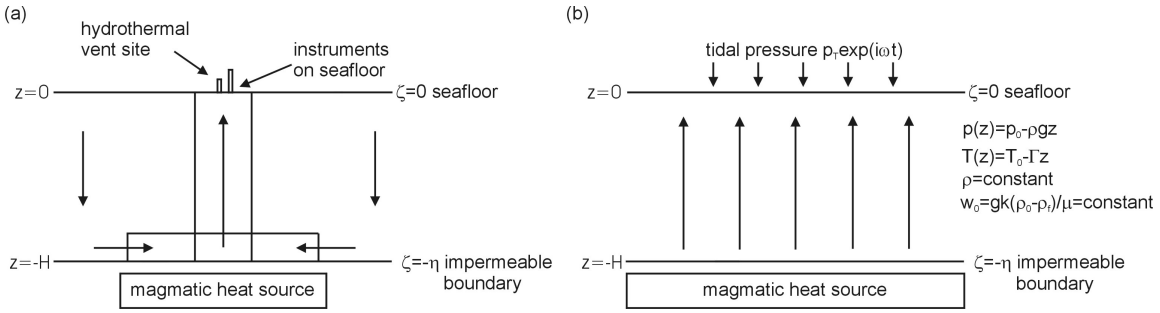

Figure 1. Schematic diagrams of a seafloor hydrothermal system. (a) A two–dimensional model with arrows showing fluid flow. Fluid descends through a 'recharge zone' into a 'reaction zone' above the heat source and then ascends through a 'discharge zone' to the seafloor. (b) A simplified one–dimensional model corresponding to the discharge zone in part (a).

The goal of the present work is to demonstrate that even for a simplified one–dimensional seafloor of uniform permeability, tidal pressure loading can lead to temporal variability in measurable hydrothermal parameters. We shall therefore focus on the possible range of values of the transport and elastic properties of the interstitial fluid.

For simplicity, we assume also that the properties of the interstitial fluid follow those of pure water. At high temperatures and low pressures the presence of solutes in briny interstitial fluids provides the potential for multiphase flow. This might have an impact on the response of the hydrological system to external pressure loading, notably through the creation of material gradients and discontinuities in the properties of the fluid at fluid phase boundaries. Over most of the p–T regime within diffuse hydrothermal systems, however, relatively cool flow paths can be expected and single phase flow would predominate. The case for a poroelastic explanation for the observed tidal variability of hydrothermal outflow is strengthened if the data can be explained adequately by a single phase flow model without the need to invoke more complicated multiphase flow regimes.

All of the physical quantities associated with the water at a fixed point in a subseafloor convection cell, such as pressure, velocity and temperature, are expected to fluctuate as a result of tidal loading. In this paper we extend the analytical solution of *Van der Kamp and Gale* (1983) and *Wang and Davis* (1996), which is concerned solely with pressure, to cover two physical quantities we commonly measure on the seafloor, i.e. the exit velocity and the temperature of hydrothermal effluent. Furthermore, we consider the additional constraint of an impermeable boundary at the base of the hydrothermal system.

2. Fundamental concepts of poroelasticity

In this section we review briefly the aspects of the theory of poroelasticity that are relevant to hydrothermal systems under load from the ocean tide [*Biot*, 1941; *Rice and Cleary*, 1976; *Van der Kamp and Gale*, 1983; *Kümpel*, 1991]. When a fluid–filled porous medium such as the ocean crust is placed under external load, it experiences changes in stress and strain. In the absence of of time–variant (such as tidal) loading, the pressure p of the fluid in the pores is invariant with time although it is expected to vary with depth. Under tidal loading, however, the pressure will be perturbed to $p + \hat{p}$ where $\hat{p}$ is the 'incremental pore pressure'.

Two bulk moduli are relevant to the behaviour of an elastic matrix. Firstly, the matrix bulk modulus K_m is the bulk modulus of the medium when the pore space is empty and is also known as the drained bulk modulus. Secondly, the grain bulk modulus K_g is the bulk modulus of the solid grains of the medium. The coefficient of effective stress α is then defined as a measure of the relative magnitude of the matrix and grain bulk moduli [*Nur and Byerlee*, 1971]:

$$\alpha = 1 - \frac{K_m}{K_g}.$$

The coefficient of effective stress is a measure of the extent to which the existence of the pore space affects the bulk modulus of the solid–fluid mixture, and is a dimensionless number in the range $[0, 1]$ since $K_m \leq K_g$.

We are concerned with the effect of tidal loading at periods of at least 12 hours. This timescale is much greater than the time taken for seismic waves (velocity > 1 km.s^{-1}), to cover the lengthscales appropriate to hydrothermal systems (< 10 km). Consequently, on the timescale of interest, the elastic stresses due to tidal loading are transmitted almost instantaneously through the solid matrix of a hydrothermal system. In the case of loading by a confining pressure p_c, it then follows from the conservation of fluid mass that the incremental pore pressure $\hat{p}$ is governed by the equation:

$$\frac{\partial \hat{p}}{\partial t} - \left[\frac{k}{\mu S}\right] \nabla^2 \hat{p} = \beta \frac{\partial p_c}{\partial t}. \qquad (1)$$

Here k is the permeability of the rock matrix and μ is the dynamic viscosity of the interstitial fluid. The storage compressibility S is defined by:

$$S = \left(K_m^{-1} - K_g^{-1}\right) + \phi \left(K_f^{-1} - K_g^{-1}\right),$$

and the Skempton ratio (or 'loading efficiency') β is defined by

$$\beta = \frac{\left(K_m^{-1} - K_g^{-1}\right)}{\left(K_m^{-1} - K_g^{-1}\right) + \phi \left(K_f^{-1} - K_g^{-1}\right)} = \frac{\alpha}{K_m S}.$$

The storage compressibility S has units of reciprocal pressure, and can be interpreted as the volume of interstitial fluid that is added to the pore space, per unit volume of porous rock, per unit increase in pore pressure [*Kümpel*, 1991]. The Skempton ratio β is a dimensionless parameter in the range $[0, 1]$. When a poroelastic medium is loaded and reaches elastic equilibrium, equation 1 has the solution $\hat{p} = \beta \hat{p}_c$. The Skempton ratio can therefore be interpreted as the proportion of the total applied stress that is borne by the pore fluid when all flow has ceased.

2.1. One–dimensional poroelasticity

The area of seafloor associated with an individual hydrothermal system typically has a lengthscale of at most 1 km. This is much smaller than the typical wavelength of the ocean tide [*Doodson and Warburg*, 1941]. Consequently, it is reasonable to suppose that, at any time, the tidal loading over the area of seafloor associated with an individual hydrothermal convection cell is uniform. In general terms, convecting fluid passes through three distinct regions in a hydrothermal cell (Figure 1*a*). Firstly, cold seawater descends through a broad 'recharge zone' towards a heat source at depth. It then becomes heated as it travels laterally though a 'reaction zone' immediately above the heat source, before ascending through a 'discharge zone' to be vented on the seafloor. The temperature limits within the cell are provided by cold seawater at $\sim 2^{\circ}$C and the heat source (assumed to be a magma chamber or dike) at $\sim 1200^{\circ}$C. For simplicity, we consider a 'one–dimensional' response to tidal loading so that the incremental pore pressure is $\hat{p}(z,t)$ (Figure 1*b*). Consequently, the poroelastic properties of the seafloor are taken to be homogeneous and it is assumed that there are no pressure gradients or strains in the horizontal directions. Conceptually, this one–dimensional model corresponds to the discharge zone of the prototypical two–dimensional convection cell of Figure 1*a*. It is, of course, a considerable simplification to treat the response of a poroelastic system as one–dimensional, but we do so in order to derive some exact analytical results that reveal the underlying physical controls of the system.

For the loading of a one–dimensional halfspace, it is possible to derive equations analogous to those given in the previous section [*Van der Kamp and Gale*, 1983]. We consider the incremental pore pressure due to loading by a single harmonic component of magnitude p_T and angular frequency ω. The seafloor boundary condition on the incremental pore pressure is given (in complex notation) by:

$$\hat{p}(0,t) = p_T \exp(i\omega t). \tag{2}$$

The tides in the open oceans generally have an amplitude of ~ 1 m, and so p_T typically has an amplitude of about 10 kPa. In the case of a one–dimensional model, Van der Kamp and Gale (1983) show that the incremental vertical stress is the same for all depths:

$$\hat{\sigma}_{33} = -p_T \exp i\omega t \quad \forall z. \tag{3}$$

and that equation 1 can be replaced by:

$$\frac{\partial \hat{p}}{\partial t} - \left[\frac{k}{\mu S_1}\right] \frac{\partial^2 \hat{p}}{\partial z^2} = -\gamma \frac{\partial \hat{\sigma}_{33}}{\partial t}. \tag{4}$$

This has the same form as equation 1 with the difference that the storage compressibility S and Skempton ratio β have been replaced by their one–dimensional analogues S_1 and γ defined by

$$S_1 = \left[\frac{3(1-\nu) - 2\alpha\beta(1-2\nu)}{3(1-\nu)}\right] S,$$

$$\gamma = \left[\frac{(1+\nu)}{3(1-\nu) - 2\alpha\beta(1-2\nu)}\right] \beta.$$

where ν is the Poisson's ratio of the matrix frame (the 'drained' Poisson's ratio). We refer to the parameter γ as the 'tidal loading efficiency'.

Since $\hat{\sigma}_{33}(z,t)$ is known from equation 3, equation 4 constitutes a forced diffusion equation for the incremental pore pressure with a diffusivity κ defined by:

$$\kappa = \left[\frac{k}{\mu S_1}\right].$$

The incremental pore pressure in a 1–d seafloor is therefore governed by the equation:

$$\frac{\partial \hat{p}}{\partial t} - \kappa \frac{\partial^2 \hat{p}}{\partial z^2} = \gamma \frac{\partial}{\partial t} \left(p_T \exp i\omega t\right). \tag{5}$$

2.2. Parameter values in a hydrothermal system

The large range of possible temperatures within a hydrothermal system (0°C to 1200°C) [*Jupp and Schultz*, 2000] leads to a large range of possible values for the fluid bulk modulus K_f (or equivalently, its reciprocal the fluid compressibility K_f^{-1}) (Figure 2). The values of the compressibility considered here are isenthalpic compressibilities defined [*Van Wylen and Sonntag*, 1978] by the equation:

$$K_f^{-1} = \frac{1}{\rho_f} \left.\frac{\partial \rho_f}{\partial p}\right|_{h=\text{constant}}$$

where the fluid has specific enthalpy h and density ρ_f.

The fluid bulk modulus is plotted as a function of pressure and temperature in Figure 2a over a range relevant to seafloor hydrothermal systems. The fluid bulk modulus depends strongly on temperature but only weakly on pressure in the regime below $\sim 400^{\circ}$C for which hydrothermal water is liquid–like. There is a sharp change in behaviour at $\sim 400^{\circ}$C as water moves from a liquid–like state to a gas–like state. At seafloor pressures, the bulk modulus of water ranges from a cold, liquid–like value of $K_f \approx 2.2$ GPa at 2°C to hot, gas–like values of $K_f \approx p$ above $\sim 400^{\circ}$C. Thus, the bulk modulus of water above $\sim 400^{\circ}$C in a hydrothermal system is approximately equal to the ambient pressure - a relationship which would be exact in the case of a perfect gas [*Van Wylen and Sonntag*, 1978].

We now consider the likely range of the poroelastic properties of the seafloor, which depend on the drained matrix bulk modulus K_m. In order to estimate typical values for K_m we suppose that the solid material of the seafloor has density $\rho_s = 3181$ kg.m^{-3} and bulk modulus $K_g = 50$ GPa [*Carmichael*, 1966]. The bulk density of the seafloor is then $\rho = \phi\rho_f + (1-\phi)\rho_s$ and poroelastic properties can be estimated by combining measurements of the P– and S–wave velocities V_p and V_s, with the Biot–Gassmann relations for the seismic properties of fluid–filled porous media [*Kent et al.*, 1993; *Murphy et al.*, 1993; *Crone and Wilcock*, 2002; *T.J. Crone, pers. comm.*, 2003]. The shear modulus G and undrained Poisson's ratio ν_u are:

$$G = \rho V_s^2; \quad \nu_u = \frac{V_p^2 - 2V_s^2}{2V_p^2 - 2V_s^2}, \tag{6}$$

and the matrix bulk modulus K_m is given by the following form of Gassmann's equation:

$$K_m = \frac{G\left[\frac{4}{3} - \frac{V_p^2}{V_s^2}\right]\left[\frac{\phi}{K_f} + \frac{1-\phi}{K_g}\right] - 1}{\frac{G}{K_g^2}\left[\frac{4}{3} - \frac{V_p^2}{V_s^2}\right] + \frac{\phi}{K_f} - \frac{1+\phi}{K_g}}. \tag{7}$$

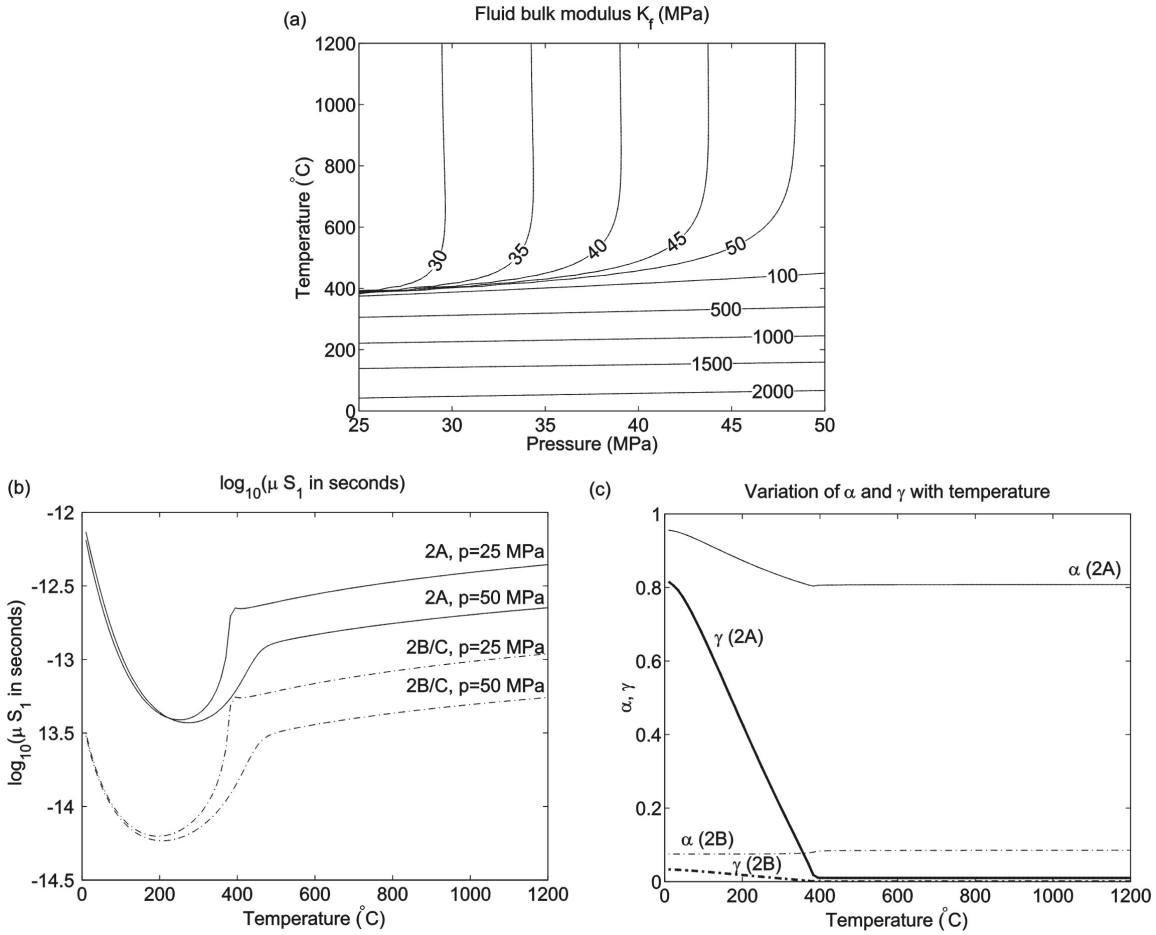

Figure 2. The range of poroelastic parameters expected in a seafloor hydrothermal system. Thermodynamic data for water are derived from the steam tables in HYDROTHERM simulation code [*Hayba and Ingebritsen*, 1994; *Haar et al.*, 1984; *Watson et al.*, 1980; *Sengers and Kamgar-Parsi*, 1984; *Sengers and Watson*, 1986]. A hydrostatic pressure of 10 MPa corresponds to a depth 1 km below sea level. (*a*) Fluid bulk modulus K_f. (*b*) The 'scaled reciprocal diffusivity' μS_1. (The true diffusivity is $\kappa = k/\mu S_1$ where k is permeability). Values are calculated using typical parameter values for the seismic layers 2A and 2B/C (equations 8 and 9) and at pressures correponding to depths 2.5 km and 5 km below sea level. (*c*) Coefficient of effective stress α and tidal loading efficiency γ with seafloor properties as in part (*b*). Curves are shown for $p = 25$ MPa.

In figure 2 we present typical seafloor properties for two illustrative cases that are relevant to seafloor hydrothermal systems. We consider 'typical' properties for the seismic layer 2A, which represents the upper few hundred metres of a typical hydrothermal system, and for seismic layers 2B and 2C which underlie layer 2A. Specifically, we calculate representative values for the poroelastic parameters based on the following data [*Christeson et al.*, 1994; *Collier and Singh*, 1998; *Barclay et al.*, 2001]:

$$\text{typical layer 2A} \quad \begin{cases} \phi &= 0.2 \\ V_p &= 2000 \text{ m.s}^{-1} \\ V_s &= 392 \text{ m.s}^{-1} \\ \nu_u &= 0.48 \end{cases} \tag{8}$$

$$\text{typical layer 2B/C} \quad \begin{cases} \phi &= 0.05 \\ V_p &= 5500 \text{ m.s}^{-1} \\ V_s &= 3368 \text{ m.s}^{-1} \\ \nu_u &= 0.2 \end{cases} \tag{9}$$

We emphasise that the undrained Poisson's ratio ν_u is a property of the fluid–solid mixture while the drained Poisson's ratio ν in the definition of the tidal loading efficiency is a property of the matrix frame. The two values for the Poisson's ratio are therefore quite different conceptually, but the numerical difference between them is likely to be small. Accordingly, we shall treat the values of ν_u given above as estimates for the approximate values of ν likely to be found in hydrothermal systems.

3. The nature of the ocean tide

Hydrothermal time–series measurements are usually taken at the seafloor in the hope that they will reveal something about the structure of the hydrological and chemical system below the seafloor. Accordingly, we consider time variations of the seafloor pressure field to be a forcing function acting on the hydrothermal system. The response of the hydrothermal system to this external forcing acts to modulate two observable output signals - the time–series of effluent temperature and effluent flow rate at the point of emission on the seafloor. Our aim, therefore, is to compare the output signals with the forcing function in order to constrain the physical properties of the hydrothermal system. In par-

ticular, we concentrate on the part of the forcing function that is caused by those processes moderated by the tides.

Tidal signals have the advantages that they are an energetic component of the seafloor pressure spectrum and occur at frequencies that are known precisely. In some cases, direct time–series measurements of the seafloor pressure field can be used to calculate the parameters of the local ocean tide, but in their absence the local ocean tide can be estimated. Direct hydrodynamic modelling of the oceans [*Le Prevost et al.*, 1994] and data from satellite altimetry [*Schrama and Ray*, 1994; *Le Prevost et al.*, 1995] have been combined with data from deep–sea and coastal tide gauges [*Egbert et al.*, 1994] to produce maps of the global ocean tide. In any case, the ocean tide at any point on the sea surface may be regarded as known. The ocean tide varies significantly from location to location, but the frequency spectra of all tidal signals share certain common features [*Schwiderski*, 1980; *Doodson and Warburg*, 1941]. All ocean tide signals have most of their spectral power in two frequency bands - the diurnal band (corresponding to a period of about 24 hours) and the semi–diurnal band (corresponding to a period of about 12 hours). In general, the semi–diurnal components of the ocean tide are somewhat larger than the diurnal components. For simplicity, we suppose that the ocean tide consists of a single semi–diurnal signal of angular frequency $\omega \approx 1.408 \cdot 10^{-4}$ rad.s^{-1}. The governing equations are linear, and so the response of the hydrothermal system to a mixture of diurnal and semi–diurnal components could be calculated by considering the two frequencies separately.

4. Analytical solutions for 1–d model

We now consider the solution of equations 3 and 4. It follows from equation 5 that the length scale associated with tidal loading at angular frequency ω is the 'skin depth' D [*Turcotte and Schubert*, 1982] defined by:

$$D = \sqrt{\frac{2\kappa}{\omega}}. \tag{10}$$

It is shown below that pressure loading due to tidal modulation of the water column leads to an evanescent, diffusive pressure signal that decays exponentially with depth beneath the seafloor. In approximate terms, the skin depth D represents the maximum depth below the seafloor to which the pore pressure would diffuse in the absence of any impermeable boundaries.

At this point it is appropriate to consider the range of values that the skin depth might take for a seafloor hydrothermal system under tidal loading. Given a semi–diurnal tidal signal of angular frequency $\omega \sim 1.4 \cdot 10^{-4}$ rad.s^{-1} we note that the skin depth can be as small as $D \sim 1.4$ m when $k = 10^{-17}$ m^2 and the fluid is at ~ 2°C. Conversely, the skin depth can be as large as $D \sim 14$ km when $k = 10^{-10}$ m^2 and the fluid is at ~ 400°C. A skin depth of 1.4 m is very much less than the typical dimensions of a seafloor convection cell ($\sim$ 1000 m) while a skin depth of 14 km is considerably larger. In the sections below we shall investigate the importance of the size of the skin depth in relation to the vertical size of the hydrothermal system. The dependence of the skin depth on angular frequency implies that the skin depths for diurnal components are greater than those for semi–diurnal components by a factor of $\sqrt{2}$.

It is helpful to define dimensionless variables by using the diffusive lengthscale D and the tidal timescale $1/\omega$:

$$\zeta = \frac{z}{D}, \quad \tau = \omega t.$$

Equation 5 can then be rewritten in terms of the dimensionless time and depth to give the governing equation for the incremental pore pressure:

$$\frac{\partial \hat{p}}{\partial \tau} - \frac{1}{2}\frac{\partial^2 \hat{p}}{\partial \zeta^2} = i\gamma p_T \exp(i\tau), \tag{11}$$

while the seafloor boundary condition of equation 2 becomes

$$\hat{p}(\zeta, \tau) = p_T \exp(i\tau) \quad \text{on} \quad \zeta = 0. \tag{12}$$

4.1. Incremental velocity

Several previous studies have been concerned with the incremental pore pressure [e.g. *Van der Kamp and Gale*, 1983; *Wang and Davis*, 1996], but relatively few have focussed on the flow of interstitial fluids that is induced by this incremental pore pressure [e.g. *Wang et al., 1999*]. In our case, the point of interest is the spatial gradient of the incremental pore pressure rather than the incremental pore pressure itself. The tidally induced incremental velocity at the seafloor is of particular interest since it can be observed by deploying specially designed instruments [e.g. *Schultz et al.*, 1996]. By Darcy's law [*Phillips*, 1991], the incremental vertical velocity (in complex notation) is:

$$\hat{w}(\zeta, \tau) = -\frac{k}{\mu}\frac{\partial \hat{p}}{\partial z} = -\frac{S_1 \omega D}{2}\frac{\partial \hat{p}}{\partial \zeta}, \tag{13}$$

where $\hat{p}(\zeta, \tau)$ is a solution of equation 11.

4.2. Solutions for incremental pressure and velocity

We suppose that a magma chamber supplies heat to the hydrothermal convection cell at a depth H below the seafloor [*Jupp and Schultz*, 2000]. It follows that there is an impermeable boundary at a dimensionless depth η defined by

$$\eta = \frac{H}{D}.$$

The incremental pore pressure is therefore the solution of equation 11 subject to the seafloor boundary condition of equation 12 and a 'no flow' boundary condition at the base of the permeable layer:

$$\hat{w} = 0 \quad \text{on} \quad \zeta = -\eta.$$

It is helpful to define the complex constant

$$\lambda = 1 + i = \sqrt{2}\exp(i\pi/4)$$

in order to give the general solution for the incremental pore pressure:

$$\begin{aligned} \hat{p}(\zeta, \tau) &= p_T \\ &\times \left[(1-\gamma)\frac{\cosh(\lambda\zeta + \lambda\eta)}{\cosh(\lambda\eta)} + \gamma\right] \\ &\times \exp i\tau. \end{aligned} \tag{14}$$

It is useful conceptually to split this solution into the sum of an instantaneous signal

$$p_T \gamma \exp(i\tau),$$

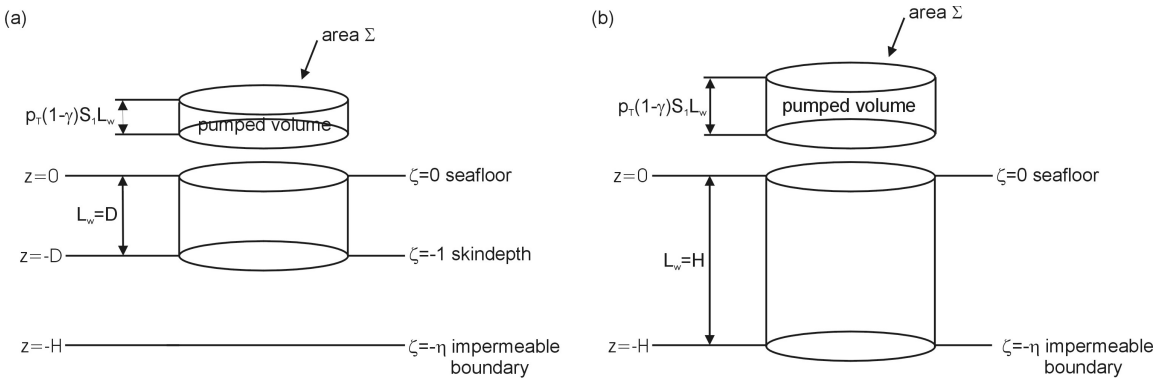

Figure 3. Sketch showing the mass of water (labelled the 'pumped volume') that would be driven into and out of the seafloor by tidal loading if the steady state upwelling velocity were zero ($w_0 = 0$). (a) In the regimes for which $\eta \gg 1$ tidal pumping is limited by the skin depth D. (b) In the regimes for which $\eta \gg 1$ tidal pumping is limited by the boundary at depth H.

and a diffusive signal

$$p_T(1-\gamma)\frac{\cosh(\lambda\zeta+\lambda\eta)}{\cosh(\lambda\eta)}\exp(i\tau).$$

The instantaneous signal is in phase with the ocean tide and has magnitude $p_T\gamma$ at all depths. Consequently, it does not produce any pressure gradients to drive vertical flow. In contrast, the diffusive pressure signal is a function of depth ζ and depends on the value of the parameter η. There are two limiting cases in which diffusive skin depth D is either much smaller or much larger than the layer depth H. When the diffusive skin depth is much smaller than the depth of the impermeable boundary (Figure 3a), $\eta \gg 1$ and the diffusive pressure signal is approximately

$$p_T(1-\gamma)\exp(\zeta)\exp(i\zeta+i\tau).$$

This is the infinite halfspace solution discussed by *Van der Kamp and Gale* (1983) and *Wang and Davis* (1996) in which an impermeable boundary lies sufficiently deeply that it does not influence the flow near the seafloor. From equation 10 we see that the skin depth decreases as the permeability decreases. In other words, provided that the permeability is sufficiently small, the diffusive pore pressure signal cannot reach the impermeable boundary at $z = -H$ and is instead limited to a depth $z = -D$. This limit is essentially the distance through which fluid can be driven by diffusive pressure gradients in the tidal timescale $\sim 1/\omega$. When $\eta \gg 1$, the diffusive pressure signal is negligible for depths significantly greater than the skin depth, and so the tidal loading efficiency γ represents the proportion of the tidal load that is borne by the interstitial fluid at sufficiently large depths.

We now consider the case when the diffusive skin depth is much larger than the depth of the permeable layer (Figure 3b). In this regime $\eta \ll 1$ and so (from equation A2) the diffusive pressure signal is approximately

$$p_T(1-\gamma)\left(1+i\eta^2\left(\frac{\zeta}{\eta}+1\right)^2\right)\exp(i\tau).$$

In this regime the depth of tidal pumping is limited by the impermeable boundary at $z = -H$. In physical terms, the permeability is sufficiently large that very small pressure gradients are required to drive fluid in and out of the permeable layer over the tidal timescale $\sim 1/\omega$. For this reason, the diffusive pore pressure in this regime varies very little between the seafloor $\zeta = 0$ and the base of the permeable layer at $\zeta = -\eta$.

Returning to the general case where η can take any value, equation 13 can be used to give the general solution for the incremental velocity:

$$\begin{aligned}\hat{w}(\zeta,\tau) &= [p_T(1-\gamma)S_1] \\ &\times\ \omega\frac{D}{\sqrt{2}}\frac{\sinh(\lambda(\zeta+\eta))}{\cosh(\lambda\eta)} \\ &\times\ \exp(i(\tau-3\pi/4)).\end{aligned} \tag{15}$$

The incremental velocity on the seafloor is of particular interest since it can be measured by seafloor instruments. It is

$$\begin{aligned}\hat{w}(0,\tau) &= [p_T(1-\gamma)S_1] \\ &\times\ \omega\frac{D}{\sqrt{2}}\tanh(\lambda\eta) \\ &\times\ \exp(i(\tau-3\pi/4)).\end{aligned} \tag{16}$$

The incremental velocity on the seafloor can therefore be written in the generic form

$$\begin{aligned}\hat{w}(0,\tau) &= [p_T(1-\gamma)S_1] \\ &\times\ \omega L_w \\ &\times\ \exp(i(\tau-\psi_w)),\end{aligned} \tag{17}$$

where L_w is a lengthscale controlling the magnitude of the velocity signal and ψ_w is an angle expressing its phase relative to the ocean tide at the seafloor. We now consider how L_w and ψ_w depend on the relative size of the layer thickness and the skin depth via the parameter η. It can be shown (from equations A3, A6 and A7) that:

$$\begin{aligned}|\tanh(\lambda\eta)| &= \sqrt{\frac{\sinh^2\eta+\sin^2\eta}{\sinh^2\eta+\cos^2\eta}} \\ &\approx \begin{cases}\sqrt{2}\eta & \text{if}\quad \eta\ll 1\\ 1 & \text{if}\quad \eta\gg 1.\end{cases}\end{aligned}$$

Equation 16 then shows that the lengthscale L_w in equation 17 is

$$\begin{aligned}L_w &= \frac{D}{\sqrt{2}}\sqrt{\frac{\sinh^2\eta+\sin^2\eta}{\sinh^2\eta+\cos^2\eta}} \\ &\approx \begin{cases}H & \text{if}\quad \eta\ll 1\\ D/\sqrt{2} & \text{if}\quad \eta\gg 1.\end{cases}\end{aligned}$$

We deduce that L_w represents the maximum depth to which fluid could be driven by the tidal loading (if the fluid in the

seafloor were otherwise at rest) and is equal to the minimum of the two lengthscales H and $D/\sqrt{2}$. When $H \ll D$, then $\eta \ll 1$ and tidal pumping is limited by the depth of the impermeable boundary H. Conversely, when $D \ll H$, then $\eta \gg 1$ and tidal pumping is limited by the diffusive lengthscale D. Since fluid penetrates in general to a depth L_w, the magnitude of the incremental velocity at the seafloor can now be interpreted in physical terms by considering the transfer of fluid across a patch of seafloor of area Σ over the course of a tidal cycle (Figure 3a) in the absence of any steady state upwelling. Below the seafloor, diffusive pore pressure oscillations of magnitude $\sim p_T(1-\gamma)$ drive a flow of water down to a depth $\sim L_w$. We recall that the storage compressibility S_1 represents the volume of water stored per unit increase in pore pressure per unit volume of rock. Thus, we require that a total volume of water $\sim p_T(1-\gamma)S_1 L_w \Sigma$ be driven through an area of seafloor Σ in a time $\sim 1/\omega$. It follows that the magnitude of the volume flux is $\sim p_T(1-\gamma)S_1\omega L_w$ as in equation 17.

We now consider the phase lag ψ_w of the incremental velocity at the seafloor. It can be shown (from equations A3, A6 and A7) that

$$\begin{aligned} \arg\left[\tanh\left(\lambda\eta\right)\right] &= \tan^{-1}\left[\frac{\sin 2\eta}{\sinh 2\eta}\right] \\ &\approx \begin{cases} \pi/4 & \text{if} \quad \eta \ll 1 \\ 0 & \text{if} \quad \eta \gg 1. \end{cases} \end{aligned}$$

It follows that the incremental velocity on the seafloor lags the ocean tide by a radian angle:

$$\begin{aligned} \psi_w &= 3\pi/4 - \tan^{-1}\left[\frac{\sin 2\eta}{\sinh 2\eta}\right] \\ &\approx \begin{cases} \pi/2 & \text{if} \quad \eta \ll 1 \\ 3\pi/4 & \text{if} \quad \eta \gg 1. \end{cases} \end{aligned}$$

The phase lag ψ_w is plotted as a function of the parameter η in Figure 4a. The phase lag of the incremental velocity can be interpreted in the limits $\eta \ll 1$ and $\eta \gg 1$.

Firstly, when the skin depth is much larger than the depth of the permeable layer, $\eta \ll 1$ and the phase lag is $\psi_w \approx \pi/2$. This means that the peak outflow from the seafloor occurs about 3 hours after high tide for semi–diurnal components and about 6 hours after high tide for diurnal components. In this regime, the permeability is sufficiently large that changes in the tidal pressure field on the seafloor are transmitted almost instantaneously in comparison with the tidal timescale $\sim 1/\omega$. Consequently, the permeable layer contains a maximum amount of poroelastically stored water at high tide, and a minimum amount at low tide. It follows that peak outflow from the seafloor occurs at the falling half–tide, which corresponds to a radian phase lag $\psi_w \approx \pi/2$.

Conversely, when the skin depth is much smaller than the depth of the permeable layer, $\eta \gg 1$ and the phase lag is $\psi_w \sim 3\pi/4$. This means that peak outflow from the seafloor occurs about 4.5 hours after high tide for semi–diurnal components and about 9 hours after high tide for diurnal components. In this regime, the impermeable boundary at $\zeta = -\eta$ has no influence on the solution and the diffusive pressure signal takes the form of a diffusive travelling wave whose amplitude decays over the diffusive lengthscale. The peak outflow from the seafloor occurs when the pressure gradient at the seafloor is greatest. As shown in Figure 4, this occurs halfway between falling half–tide and low tide, at a radian phase angle $\psi_w = 3\pi/4$ (Table 1).

4.3. Incremental temperature

We have so far considered the incremental pore pressure $\hat{p}(\zeta,\tau)$ and its spatial gradient - the incremental velocity $\hat{w}(\zeta,\tau)$. We now consider a third quantity of interest: the incremental temperature $\hat{T}(\zeta,\tau)$. We motivate this discussion by recalling that the incremental temperature of hydrothermal effluent $\hat{T}(0,\tau)$ is often measured by researchers from the point of emission on the seafloor.

For simplicity, we suppose that the permeable layer of depth H contains hot water driven upwards by buoyancy. In a real system there is expected to be a thin region of lateral flow (the 'reaction zone') just above the impermeable boundary, which feeds the upwelling fluid (Figure 1a). Our assumption of one–dimensional geometry, however, means that we must ignore this flow and we consider instead the idealised case of uniform vertical flow throughout the permeable layer. We suppose that, in the absence of tidal loading, pressure and temperature are linear functions of depth throughout the permeable layer (Figure 1b). We expect the pressure gradient to be cold hydrostatic (so that the fluid ascends under buoyancy forces) and we denote the temperature gradient by Γ. The existence of a vertical temperature gradient means that fluid must cool as it ascends towards the seafloor. There are two mechanisms by which fluid cools in a real system - (1) conductively and (2) adiabatically (i.e. without losing any heat) because of depressurisation on ascent. Lateral conductive heat losses cannot be incorporated into this model because it is one–dimensional, while vertical conductive losses are negligible in a thermal plume [*Phillips*, 1991]. We suppose therefore that the steady state temperature gradient Γ is caused by adiabatic cooling alone. This is probably a reasonable approximation for a real seafloor system [*Bischoff and Rosenbauer*, 1985]. If a hydrothermal vent field lies 2.5 km below sea level and the reaction zone lies a further 1 km below the seafloor, then the upwelling fluid depressurises from ~ 35 MPa to ~ 25 MPa during its ascent through the discharge zone. Under adiabatic cooling alone, water leaving the reaction zone at $\sim 400^{\circ}$C would cool to $\sim 352^{\circ}$C on ascent to the seafloor [*Haar et al.*, 1984], suggesting that an adiabatic temperature gradient $\Gamma \sim 0.05$ K.m^{-1} is probably typical.

The steady state pressure and temperature are taken to be

$$p(z) = p_0 - \rho_0 g z, \quad T(z) = T_0 - \Gamma z.$$

We suppose for simplicity that the density ρ_f and dynamic viscosity μ of the water do not vary with depth. The buoyancy–driven vertical Darcy velocity (in the absence of tidal loading) therefore has the constant value:

$$w_0 = -\frac{k}{\mu}\left[\frac{\mathrm{d}p}{\mathrm{d}z} + \rho_f g\right] = \frac{gk\left(\rho_0 - \rho_f\right)}{\mu}.$$

In general, flow with Darcy velocity w_0 advects temperature signals at a speed rw_0 where the dimensionless ratio $r = \rho_f c_f/\rho c$ is typically of order 1 [*Turcotte and Schubert*, 1982]. Here $\rho_f c_f$ is the volumetric heat capacity of the water and ρc is the volumetric heat capacity of the water–rock mixture. For simplicity, we assume here that $r = 1$, although we retain the term in the equations for generality.

We now suppose that the steady, one–dimensional solution of equation 4.3 is disturbed by tidal loading at angular frequency ω. This leads to the introduction of a new lengthscale

$$A = \frac{rw_0}{\omega},$$

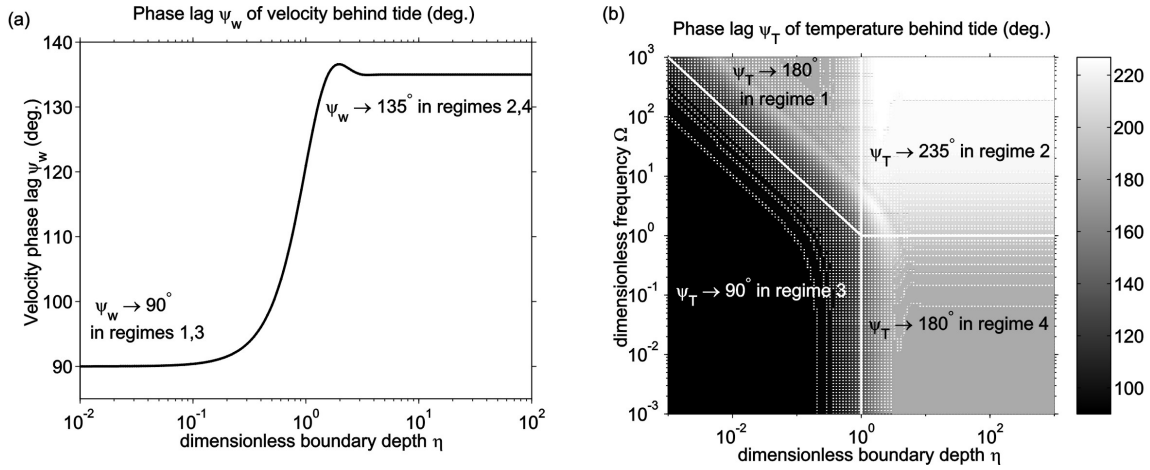

Figure 4. The predicted phase lag of the incremental velocity ψ_w and of the incremental temperature ψ_T behind the ocean tide at the seafloor as functions of the dimensionless parameters η and Ω. (a) The velocity phase lag ψ_w. (b) The temperature phase lag ψ_T.

Table 1. Summary of the approximate solutions in the limiting regimes

Regime	Approximate Solutions	Lengthscale	Phase lag
1	$\hat{p} \approx p_T \left[1 + (1-\gamma)\eta^2 \left(\frac{\zeta}{\eta} + 1\right)^2 i\right] \exp(i\tau)$		
	$\hat{w} \approx [p_T(1-\gamma)S_1]\, \omega H \left(\frac{\zeta}{\eta} + 1\right) \exp(i(\tau - \pi/2))$	$L_w = H$	$\psi_w = \pi/2$
	$\hat{T} \approx [p_T(1-\gamma)S_1]\, r\Gamma H \left(\frac{\zeta}{\eta} + 1\right) \exp(i(\tau - \pi))$	$L_T = H$	$\psi_T = \pi$
2	$\hat{p} \approx p_T(1-\gamma)\exp(\zeta)\exp(i(\zeta+\tau)) + p_T\gamma\exp(i\tau)$		
	$\hat{w} \approx [p_T(1-\gamma)S_1]\, \omega \frac{D}{\sqrt{2}} \exp(\zeta)\exp\left(i(\zeta + \tau - 3\pi/4)\right)$	$L_w = D/\sqrt{2}$	$\psi_w = 3\pi/4$
	$\hat{T} \approx [p_T(1-\gamma)S_1]\, r\Gamma \frac{D}{\sqrt{2}} \exp(\zeta)\exp\left(i(\zeta + \tau - 5\pi/4)\right)$	$L_T = D/\sqrt{2}$	$\psi_T = 5\pi/4$
3	$\hat{p} \approx p_T \left[1 + (1-\gamma)\eta^2 \left(\frac{\zeta}{\eta} + 1\right)^2 i\right] \exp(i\tau)$		
	$\hat{w} \approx [p_T(1-\gamma)S_1]\, \omega H \left(\frac{\zeta}{\eta} + 1\right) \exp\left(i(\tau - \pi/2)\right)$	$L_w = H$	$\psi_w = \pi/2$
	$\hat{T} \approx [p_T(1-\gamma)S_1]\, r\Gamma \frac{H^2}{2A} \left(\frac{\zeta}{\eta} + 1\right)^2 \exp\left(i(\tau - \pi/2)\right)$	$L_T = H^2/2A$	$\psi_T = \pi/2$
4	$\hat{p} \approx p_T(1-\gamma)\exp(\zeta)\exp(i(\zeta+\tau)) + p_T\gamma\exp(i\tau)$		
	$\hat{w} \approx [p_T(1-\gamma)S_1]\, \omega \frac{D}{\sqrt{2}} \exp(\zeta)\exp\left(i(\zeta + \tau - 3\pi/4)\right)$	$L_w = D/\sqrt{2}$	$\psi_w = 3\pi/4$
	$\hat{T} \approx [p_T(1-\gamma)S_1]\, r\Gamma \frac{D^2}{2A} \exp(\zeta)\exp(i(\zeta + \tau - \pi))$	$L_T = D^2/2A$	$\psi_T = \pi$

which we term the 'advection lengthscale' since it represents the distance over which the steady background flow can advect thermal signals at speed rw_0 during the tidal timescale $1/\omega$. We remark at this stage that we might expect the incremental temperature to depend on the relative magnitudes of the three lengthscales inherent to the problem: the layer thickness H, the diffusive skin depth D and the advective lengthscale A. We suppose that the pressure, velocity and temperature are perturbed from their steady state values as follows:

$$\begin{aligned} p(z) &\rightarrow p_0 - \rho_f g z + \hat{p}(z,t), \\ w_0 &\rightarrow w_0 + \hat{w}(z,t), \\ T(z) &\rightarrow T_0 - \Gamma z + \hat{T}(z,t). \end{aligned}$$

Assuming that the incremental pressure $\hat{p}(z,t)$ and incremental velocity $\hat{w}(z,t)$ are given by the 1–d solutions discussed in the previous section (equations 14 and 15), an expression for the incremental temperature $\hat{T}(z,t)$ can be derived. Assuming that tidally–induced changes in fluid density and adiabatic cooling are negligible, the conservation of energy under tidal loading is expressed by the equation:

$$\frac{\partial}{\partial t}\left(T + \hat{T}\right) + r\left(w_0 + \hat{w}\right)\frac{\partial}{\partial z}\left(T + \hat{T}\right) = -r\Gamma w_0,$$

where the term on the right hand side represents the rate at which upwelling fluid is cooled adiabatically. This equation can be linearised by neglecting the product of any two incremental properties. Rewriting the linearised equation in terms of the dimensionless coordinates ζ and τ gives the governing equation for the incremental temperature:

$$\frac{\partial \hat{T}}{\partial \tau} + \left[\frac{1}{\Omega}\right]\frac{\partial \hat{T}}{\partial \zeta} = \left[\frac{r\Gamma}{\omega}\right]\hat{w}, \tag{18}$$

where we define the dimensionless frequency Ω as follows:

$$\Omega = \frac{\omega D}{r w_0} = \frac{D}{A}.$$

The parameter Ω is therefore the ratio of the skin depth D to the advective lengthscale A. We now suppose that the heat source driving the hydrothermal system from below has sufficient thermal inertia that the temperature is held constant at the base of the permeable layer when the system is loaded by the tide. It follows that equation 18 must be solved subject to the boundary condition

$$\hat{T} = 0 \text{ on } \zeta = -\eta.$$

Assuming that the incremental velocity solution is given by equation 15, we deduce that the incremental temperature is

$$\begin{aligned}\hat{T}(\zeta,\tau) &= [p_T\,(1-\gamma)\,S_1] \\ &\times\ r\Gamma\frac{D}{\sqrt{2}}\left[\frac{\Omega\lambda\cosh(\lambda(\zeta+\eta))}{(\Omega^2+\lambda^2)\cosh(\lambda\eta)}\right. \\ &-\ \frac{\Omega\lambda\exp(-i\Omega(\zeta+\eta))}{(\Omega^2+\lambda^2)\cosh(\lambda\eta)} \\ &-\ \left.\frac{i\Omega^2\sinh(\lambda(\zeta+\eta))}{(\Omega^2+\lambda^2)\cosh(\lambda\eta)}\right] \\ &\times\ \exp\left(i(\tau-3\pi/4)\right).\end{aligned}$$

It follows that the incremental temperature on the seafloor is

$$\begin{aligned}\hat{T}(0,\tau) &= [p_T\,(1-\gamma)\,S_1] \\ &\times\ r\Gamma\frac{D}{\sqrt{2}}\left[\frac{\Omega\lambda}{(\Omega^2+\lambda^2)}\right. \\ &-\ \frac{\Omega\lambda\exp(-i\Omega\eta)}{(\Omega^2+\lambda^2)\cosh(\lambda\eta)} \\ &-\ \left.\frac{i\Omega^2}{(\Omega^2+\lambda^2)}\tanh(\lambda\eta)\right] \\ &\times\ \exp\left(i(\tau-3\pi/4)\right).\end{aligned}$$

By analogy with equation 17, the incremental temperature on the seafloor can be written in the generic form:

$$\begin{aligned}\hat{T}(0,\tau) &= [p_T\,(1-\gamma)\,S_1] \\ &\times\ r\Gamma L_T \\ &\times\ \exp\left(i(\tau-\psi_T)\right),\end{aligned}$$

where L_T is a lengthscale controlling the magnitude of the temperature signal and ψ_T is an angle expressing its phase relative to the ocean tide at the seafloor. The lengthscale L_T and the phase lag ψ_T are functions of the two dimensionless parameters η and Ω.

In order to gain insight into the underlying physics, we now consider approximate solutions for the incremental temperature when the dimensionless parameters η and Ω take extreme values (Table 1).

Firstly, we consider the case where Ω is 'large'. In physical terms, we demand that Ω be sufficiently large that the tidal timescale is much smaller than the time taken for the background flow to advect temperature changes over the fluid penetration depth L_w. We recall from equation 17 that $L_w \approx H$ for $\eta \ll 1$ and $L_w \approx D/\sqrt{2}$ for $\eta \gg 1$. Hence the 'large Ω' regime can be defined as that for which $A \ll L_w$. We label the 'large Ω' regimes as follows:

$$\begin{aligned}&\text{Regime 1}: \ \eta \ll 1, \ \ \Omega\eta \gg 1 \\ &\text{Regime 2}: \ \eta \gg 1, \ \ \Omega \gg 1\end{aligned}$$

When Ω is large, equation 18 can be replaced by the approximation

$$\frac{\partial\hat{T}}{\partial\tau} \approx \left[\frac{r\Gamma}{\omega}\right]\hat{w} \quad \text{in regimes } 1,2,$$

and so the rate of change of the incremental temperature balances the incremental velocity. Since all incremental quantities are sinusoidal in time, it follows that the incremental temperature must lag the incremental velocity by a radian angle $\pi/2$. Thus $\psi_T = \psi_w + \pi/2$ in regimes 1 and 2.

Similarly, we can define 'small Ω' regimes to be those for which the tidal timescale is much larger than the time taken for the background flow to advect temperature changes over the fluid penetration depth L_w. Hence we define the 'small Ω' regimes to be those for which $A \gg L_w$ and we label them as follows:

$$\begin{aligned}&\text{Regime 3}: \ \eta \ll 1, \ \ \Omega\eta \ll 1 \\ &\text{Regime 4}: \ \eta \gg 1, \ \ \Omega \ll 1\end{aligned}$$

In these regimes, equation 18 can be replaced by the approximation

$$\frac{\partial\hat{T}}{\partial\zeta} \approx \Omega\left[\frac{r\Gamma}{\omega}\right]\hat{w} \quad \text{in regimes } 3,4, \tag{19}$$

and so it is now the spatial derivative of the incremental temperature that balances the incremental velocity. In order to derive the temperature phase lag ψ_T, regimes 3 and 4 must be considered separately.

In regime 3, equation 15 can be replaced by the approximation

$$\hat{w} \approx [p_T(1-\gamma)S_1]\,\omega H\left(\frac{\zeta}{\eta}+1\right)\exp(i(\tau-\pi/2)).$$

Equation 19 then implies that

$$\hat{T} \approx [p_T(1-\gamma)S_1]\,r\Gamma\frac{H^2}{2A}\left(\frac{\zeta}{\eta}+1\right)^2\exp(i(\tau-\pi/2)).$$

It follows that there is no phase lag between the velocity and temperature signals at the seafloor in regime 3 and so $\psi_T = \psi_w = \pi/2$.

In regime 4, on the other hand, equation 15 can be replaced by the approximation

$$\hat{w} \approx [p_T(1-\gamma)S_1]\,\omega\frac{D}{\sqrt{2}}\exp(\zeta)\exp(i(\zeta+\tau-3\pi/4)).$$

It follows from equation 19 that

$$\hat{T} \approx [p_T(1-\gamma)S_1]\,r\Gamma\frac{D^2}{2A}\exp(\zeta)\exp(i(\zeta+\tau-\pi)),$$

and so there is a phase lag of $\pi/4$ radians between the velocity and temperature signals. Thus $\psi_w = 3\pi/4$ and $\psi_T = \pi$ in regime 4.

5. Application of solution to a typical hydrothermal system

In the section above we derived the general solution for tidal loading of a one–dimensional seafloor containing upwelling fluid. We showed that the nature of the solution depends on the values of the dimensionless parameters η and Ω and we derived approximate solutions in the 4 regimes that arise when these parameters are very large or very small.

We now consider the values that η and Ω might be expected to take for a typical seafloor hydrothermal system. Accordingly we consider a hypothetical system where the seafloor lies 2.5 km below sea level and so the hydrostatic pressure at the seafloor is 250 bar or $p = 25$ MPa. We suppose that the magmatic heat source lies 1 km below the seafloor and so the depth of the impermeable boundary is $H = 1000$ m. We consider semi–diurnal tidal loading at angular frequency $\omega = 1.4 \cdot 10^{-4}$ rad.s^{-1}, and suppose that the grain bulk modulus is $K_g = 50$ GPa. The remaining elastic properties of the seafloor are then calculated from equations 6 and 7 using the typical parameters for layer 2A and layer 2B/C (equations 8 and 9). The only remaining uncertainty lies in the temperature T of the interstitial fluid and the permeability k of the seafloor. Accordingly, we plot

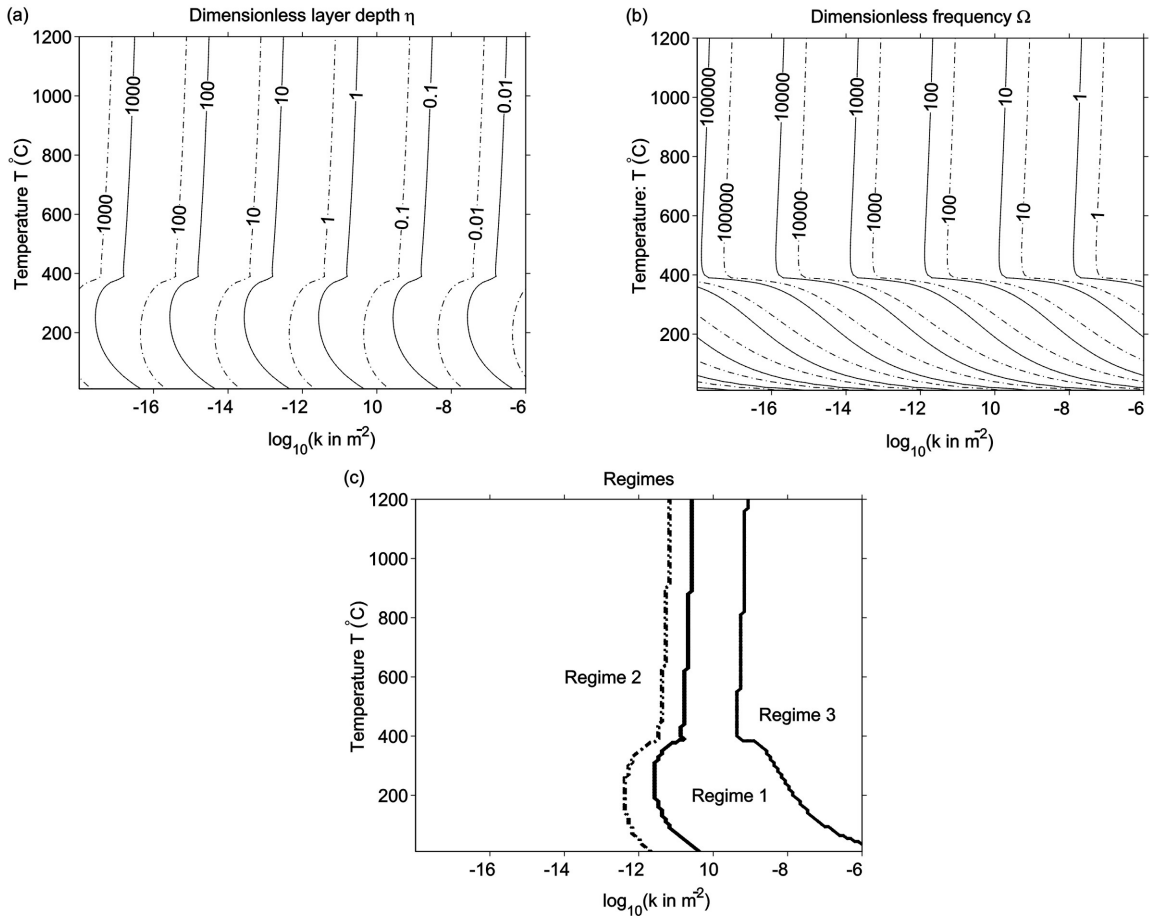

Figure 5. Diagram showing how the solution depends on temperature T and permeability k, with $K_g = 50$ GPa, $p = 25$ MPa, $H = 1000$ m and typical parameters for seismic layers 2A (equations 8 - shown here as solid lines) and 2B/C (equation 9 - shown here by dashed lines). (a) Dimensionless boundary depth η. Note logarithmic scales for k and η. (b) Dimensionless frequency Ω for $\omega = 1.4 \cdot 10^{-4}$ rad.s^{-1} (semi–diurnal tidal loading). Note logarithmic scales for k and Ω. (c) The boundaries of the limiting solution regimes, using values of η and Ω from (a) and (b). Note logarithmic scale for k. The boundaries between Regimes 1 and 2 differ for layer 2A (solid) and layer 2B/C (dashed), but the boundaries between Regimes 1 and 3 are essentially the same.

the dimensionless parameters η and Ω as functions of permeability and fluid temperature in Figure 5. In general, the permeability of the seafloor is very poorly constrained. A value of $k = 10^{-14}$ m^2 might be considered typical for a hydrothermal system [*Fisher*, 1998] but the presence of cracks could easily raise the permeability by many orders of magnitude. For completeness, we consider seafloor permeabilities ranging from a very low value of $k = 10^{-18}$ m^2 to a very high value of $k = 10^{-6}$ m^2.

Figure 5a shows that η increases as the permeability increases and could plausibly be either much greater than or much less than unity in a seafloor hydrothermal system. When $\eta \ll 1$ the skindepth D is larger than the dimensions of the hydrothermal system and tidal loading of a one–dimensional seafloor may not be sufficient to capture all of the relevant flow. If a one–dimensional model is valid, however, an empirical measurement of the velocity phase lag ψ_w could be used to constrain η (from Figure 4a) and hence the permeability of the hydrothermal system (from Figure 5a).

Figure 5b shows that our model predicts that Ω is probably greater than unity in a seafloor hydrothermal system, implying that the system is unlikely to be in regime 4 (Figure 4b). We stress, however, that our model assumes that fluid and rock are in thermal equilibrium. This is probably true deep in the system but may not apply for crack–dominated flow near the surface if fluid and rock are unable to equilibrate thermally over the daily timescale. In this case the effective value of the advective lengthscale A would increase and the effective value of Ω could be significantly smaller.

Finally, Figure 5c shows the regimes into which the hypothetical hydrothermal system falls, using the values of η and Ω from Figures 5a,b. Our model suggests that a typical hydrothermal system is probably in regime 2, although the presence of cracks might raise the permeability sufficiently for regime 1 to hold sway. For exceptionally high permeabilities characteristic of crack–dominated systems, it would be possible for the system to be in regime 3. However, the frequency of tidal loading is sufficiently large that regime 4 is inaccessible given the seafloor properties assumed here.

6. The limitations of a 1–d model

The model presented above has the advantage that it produces well defined analytical solutions that aid understanding of the basic physics. It cannot, however, reproduce all of the phenomena relevant to a real hydrothermal system.

In particular, the assumption of a one–dimensional seafloor prevents any tidally–induced horizontal flow, and the assumption of uniform fluid properties prevents a discussion of how the temperature distribution inside a real convection cell might complicate the flow. In a real hydrothermal system, the width of the discharge zone is probably a few hundred metres [e.g. *Cann and Strens*, 1989; *Delaney et al.*, 1992] and so the one–dimensional model developed here is probably inappropriate when $\eta \ll 1$ and the diffusive lengthscale exceeds the width of the discharge zone. Nonetheless, the principles uncovered by this one–dimensional analysis do allow a qualitative discussion of how spatial variations in fluid properties might influence the poroelastic response of a two– or three–dimensional hydrothermal system.

We now consider briefly how the poroelastic parameters of the interstitial fluid might be expected to vary spatially within a hydrothermal system. Jupp and Schultz (2000) present numerical simulations of subseafloor convection in which the thermodynamic properties of water impose a particular temperature structure on the convection cell. Temperatures above $\sim 400°$C are confined to the reaction zone at the base of the system, while the upwelling fluid in the discharge zone has a temperature of at most $\sim 400°$C. Based on the model of Jupp and Schultz (2000) we deduce that there is likely to be a sharp contrast in the elastic properties of the interstitial fluid at the boundary of the reaction zone where the fluid changes from the liquid–like state to the gas–like state.

The tidal loading efficiency γ represents the proportion of the applied stress borne that is borne by the interstitial fluid (for one–dimensional loading, sufficiently far from the diffusive effects near the seafloor). It follows that uniform tidal loading at the seafloor could create incremental pore pressures at depth that differ between the hot and cold parts of a hydrothermal convection cell. In general terms, when the ocean tide is high, cold regions of the cell (where γ is large) will have greater pore pressures than hot regions (where γ is small). Consequently, fluid might be expected to flow from cold regions to hot regions at high tide. The pressure difference driving this flow will be particularly large if the hot fluid is gas–like ($>\sim 400°$C) and the cold fluid is liquid–like ($<\sim 400°$C). The magnitude of the induced flow is determined by the spatial gradient of the incremental pore pressure. Consequently, the induced tidally modulated flow is expected to be large where spatial gradients in temperature are large.

7. Conclusions

We have applied the theory of poroelasticity to the tidal loading of a hydrothermal convection cell. In the present work we have considered a baseline one–dimensional model in which the tidally–loaded region is filled with uniformly upwelling fluid. We have modelled the influence of an impermeable boundary below the seafloor and have obtained general solutions for the tidally induced changes in temperature and velocity. The model is deliberately simplistic in order to elucidate physical principles.

Three important lengthscales emerge from our analysis: the depth of the impermeable boundary H, the diffusive skin depth D, and the advective lengthscale A over which thermal signals are carried by the background flow during a tidal cycle. The relative magnitudes of these three lengthscales are expressed by the dimensionless parameters η and Ω.

We have derived expressions for the magnitude and phase lag of the velocity and temperature signals at the seafloor as functions of the dimensionless parameters. The tidally–induced velocity is controlled by the depth L_w to which fluid could be driven by tidal loading in the crust. This depth is essentially the smaller of the two lengthscales D and H. The relationship of the tidally–induced temperature to the tidally–induced velocity is controlled by relative magnitude of the advective lengthscale A to this penetration depth.

We have shown that the 1–d system modelled here falls into one of 4 regimes when the parameters η and Ω are either very small or very large (Table 1). A key result of this work is that careful analysis of time–series of observable seafloor hydrothermal properties - specifically effluent temperature and flow rate - can in principle provide important diagnostic information about the thickness and permeability of the sub–seafloor hydrological system underlying seafloor venting sites.

The phase lags between the observed temperature and velocity signals and the corresponding component of the ocean tide can reveal which poroelastic regime (e.g. thick or thin, permeable or impermeable) is pertinent to a particular hydrothermal system. This development has motivated further work into the practical application of such phase information on the investigation of sub–seafloor hydrology.

The methods required for accurate analysis of the signal phase lags will be reported in a subsequent work.

Appendix A: Hyperbolic functions

We make use of the following hyperbolic functions of complex argument z,

$$\sinh(z) = \frac{\exp(z) - \exp(-z)}{2} \tag{A1}$$

$$\cosh(z) = \frac{\exp(z) + \exp(-z)}{2} \tag{A2}$$

$$\tanh(z) = \frac{\sinh(z)}{\cosh(z)} \tag{A3}$$

We make use of the trigonometric identities:

$$\cosh^2(z) = 1 + \sinh^2(z) \tag{A4}$$

$$\cos^2(z) + \sin^2(z) = 1 \tag{A5}$$

When $z = x + iy$ the following identities apply:

$$\cosh(x + iy) = \cosh(x)\cos(y) + i\sinh(x)\sin(y) \tag{A6}$$

$$\sinh(x + iy) = \sinh(x)\cos(y) + i\cosh(x)\sin(y) \tag{A7}$$

Notation

A	advective lengthscale $A = rw_0/\omega$ (m)
c_f	heat capacity (water) (J.kg^{-1}.K^{-1})
c	heat capacity (water-rock mixture) (J.kg^{-1}.K^{-1})
D	diffusive skin depth $D = \sqrt{2\kappa/\omega}$ (m)
h	specific enthalpy of water (J.kg^{-1})
H	depth of impermeable boundary (m)
k	permeability (m^2)
K_f	fluid bulk modulus (Pa)
K_g	grain bulk modulus (Pa)

K_m	matrix (drained) bulk modulus (Pa)
L_T	lengthscale for incremental temperature (m)
L_w	lengthscale for incremental velocity (m)
p	steady state pore pressure (Pa)
p_T	magnitude of ocean tide (Pa)
$\hat{p}$	incremental pore pressure (Pa)
$\hat{p}_c$	confining pressure due to tidal loading (Pa)
r	ratio of heat capacities $r = \rho_f c_f / \rho c$
S	storage compressibility (Pa^{-1})
S_1	storage compressibility for 1-d loading (Pa^{-1})
T	steady state temperature (°C)
$\hat{T}$	incremental temperature (°C)
w_0	steady vertical Darcy velocity ($\mathrm{m.s}^{-1}$)
$\hat{w}$	incremental vertical Darcy velocity ($\mathrm{m.s}^{-1}$)
α	co-efficient of effective stress
β	Skempton ratio
γ	tidal loading efficiency
Γ	background temperature gradient ($^\circ\mathrm{C.m}^{-1}$)
ζ	dimensionless vertical coordinate
η	dimensionless layer depth $\eta = H/D$
κ	diffusivity of pore pressure $\kappa = k/\mu S_1$ ($\mathrm{m}^2\mathrm{.s}^{-1}$)
λ	complex constant $\lambda = 1 + i$
μ	dynamic viscosity (Pa.s)
ν	drained Poisson's ratio
ν_u	undrained Poisson's ratio
ρ_f	density (water) ($\mathrm{kg.m}^{-3}$)
ρ	density (water-rock mixture) ($\mathrm{kg.m}^{-3}$)
$\hat{\sigma}_{ij}$	incremental stress due to tidal loading (Pa)
τ	dimensionless time $\tau = \omega t$
ϕ	porosity
ψ_T	phase lag of temperature signal (rad or °)
ψ_w	phase lag of temperature signal (rad or °)
ω	tidal frequency ($\mathrm{rad.s}^{-1}$)
Ω	dimensionless frequency $\Omega = D/A$

Acknowledgments. T.J. acknowledges support from the Newton Trust, the BP Institute and NERC studentship number GT4/96/54/E. A.S. acknowledges support from NSF grant OCE9901563, through Woods Hole Oceanographic Institution subcontract A100110 with Earth-Ocean Systems Ltd. We thank Associate Editor Kelin Wang, William Wilcock and an anonymous reviewer for helpful comments on an initial draft of this paper. We also thank Tim Crone for helpful discussions about inferring elastic properties of the crust.

References

Barclay, A.H., Toomey, D.R. and S.C. Solomon, Microearthquakes characteristics and crustal VP/VS structure at the Mid-Atlantic Ridge 35°N, *J. Geophys. Res., 106*(B2), 2017 - 2034, 2001.

Biot, M.A., General theory of three–dimensional consolidation, *J. Appl. Phys., 12*, 155 - 164, 1941.

Bischoff, J.L. and R.J. Rosenbauer, An empirical equation of state for hydrothermal seawater (3.2 percent NaCl), *Amer. J. Sci., 285*, 725 - 763, 1985.

Cann, J.R. and M.R. Strens, Modeling periodic megaplume emission by black smoker systems, *J. Geophys. Res., 94*(B9), 12227 - 12237, 1989.

Carmichael, R.S., *Handbook of Physical Properties of Rocks, II*, 345 pp., (CRC press, Boca Raton, Florida), 1966.

Chevaldonné, P, Desbruyères, D. and M. Le Haître, Time-series of temperature from three deep-sea hydrothermal vent sites, *Deep-Sea Res., 38*(11), 1417 - 1430, 1991.

Christeson, G.L., Purdy, G.M. and G.J. Fryer, Seismic constraints on shallow crustal emplacement, *J. Geophys. Res., 99*(B9), 17957 - 17973, 1994.

Collier, J.S. and S.C. Singh, Poisson's ratio structure of young oceanic crust, *J. Geophys. Res., 103*(B9), 20981 - 20996, 1998.

Cooper, M.J., *Geochemical investigations of hydrothermal fluid flow at mid-ocean ridges*, Ph.D. thesis, University of Cambridge, 218 pp., 1999.

Copley, J.T.P., Tyler, P.A., Van Dover, C.L., Schultz, A., Dickson, P., Singh, S. and M. Sulanowska, Subannual temporal variation in faunal distributions at the TAG hydrothermal mound (26°N, Mid-Atlantic Ridge), *Marine Ecology, 20*, 291 - 306, 1999.

Crone, T.J. and W.S. Wilcock, Modeling the Effects of Tidal Loading on Hydrothermal Discharge at Mid-Ocean Ridges, *Eos Trans. AGU, 83*(47), Fall Meet. Suppl., Abstract H21B-0808, 2002.

Davis, E.E. and K. Becker, Formation temperatures and pressures in a sedimented rift hydrothermal system: 10 months of CORK observations, holes 857D and 858G, *Proc. ODP, Scientific Results, 139*, 649 - 666, 1994.

Davis, E.E., Becker, K., Wang, K. and B. Carson, Long-term observations of pressure and temperature in hole 892B, Cascadia accretionary prism, *Proc. ODP, Scientific Results, 146*, 299 - 311, 1995.

Davis, E.E. and K. Becker, Tidal pumping of fluids within and from the oceanic crust: new observations and opportunities for sampling the crustal hydrosphere, *Earth Planet. Sci. Lett., 172*, 141 - 149, 1999.

Delaney, J.R., Robigou, V., McDuff, R.E. and Tivey, M.K., Geology of a vigorous hydrothermal system on the Endeavour Segment, Juan de Fuca Ridge, *J. Geophys. Res., 97*(B13), 19663 - 19682, 1992.

Delaney, J.R., Kelley, D.S., Lilley, M.D., Butterfield, D.A., McDuff, R.E. and J.A. Baross, Temporal/spatial exploration of physical, chemical and biological linkages in a submarine hydrothermal laboratory: the Endeavour Ridge, *Eos, Trans. AGU*, Fall Supplement, 1997.

Doodson, A.T. and H.D. Warburg, *Admiralty Manual of Tides*, Her Majesty's Stationery Office, 1941.

Egbert, G.D., Bennett, A.F. and M.G.G. Foreman, TOPEX / POSEIDON tides estimated using a global inverse model, *J. Geophys. Res., 99*(C12), 24821 - 24852, 1994.

Fisher, A.T., Becker, K. and E.E. Davis, The permeability of young oceanic crust east of Juan de Fuca Ridge determined using borehole thermal measurements, *Geophys. Res. Lett., 24*(11), 1311 - 1314, 1997.

Fisher, A.T., Permeability within basaltic ocean crust, *Rev. Geophys., 36*(2), 143 - 182, 1998.

Fornari, D.J., Shank, T., Von Damm, K.L., Gregg, T.K.P., Lilley, M., Levai, G., Bray, A., Haymon, R.M., Perfit, M.R. and R. Lutz, Time-series measurements at high temperature hydrothermal vents, East Pacific Rise $9°49' - 51'$N: evidence for monitoring a crustal cracking event, *Earth Plan. Sci. Lett., 160*, 419 - 431, 1998.

Fujioka, K., Kobayashi, K., Kato, K., Aoki, M., Mitsuzawa, K., Kinoshita, M. and A. Nishizawa, Tide-related variability of TAG hydrothermal activity observed by deep-sea monitoring system and OBSH, *Earth Plan. Sci. Lett., 153*, 239 - 250, 1997.

Haar, L., Gallagher, J.S. and G.S. Kell, *NBS/NRC Steam Tables*, 320pp. (Hemisphere, New York), 1984.

Hayba, D.O. and S.E. Ingebritsen, The computer model HYDROTHERM, a three–dimensional finite–difference model to simulate ground-water flow and heat transport in the temperature range of 0 to 1,200 degrees Celsius, *U.S. Geological Survey Water-Resources Investigations Report, 94-4045*, 1994.

Johnson, H.P. and V. Tunnicliffe, Time-series measurements of hydrothermal activity on northern Juan de Fuca Ridge, *Geophys. Res. Lett., 12*(10), 685 - 688, 1985.

Johnson, K.S., Childress, J.J., Beehler, C.L. and C.M. Sakamoto, Biogeochemistry of hydrothermal vent mussel communities: the deep-sea analogue to the intertidal zone, *Deep-Sea Res. I, 41*(7), 993 - 1011, 1994.

Jupp, T. and A. Schultz, A thermodynamic explanation for black smoker temperatures, *Nature, 403*, 880 - 883, 2000.

Kadko, D., Time-series gamma spectrometry of diffuse flow from the North Cleft segment of the Juan de Fuca Ridge, *Eos, Trans. AGU, Fall Meet. Suppl., 75*, 307, 1994.

Kent, G.M., Harding, A.J. and J.A. Orcutt, Distribution of magma beneath the East Pacific Rise between the Clipperton transform and the 9°17′N deval from forward modeling of common depth point data, *J. Geophys. Res., 98*(B8), 13945 - 13969, 1993.

Kinoshita, M., Matsubayashi, O. and R.P. Von Herzen, Subbottom temperature anomalies detected by long-term temperature monitoring at the TAG hydrothermal mound, *Geophys. Res. Lett., 23*(23), 3467 - 3470, 1996.

Kinoshita, M., Von Herzen, R.P., Matsubayashi, O. and K. Fujioka, Erratum to 'Tidally-driven effluent detected by long-term temperature monitoring at the TAG hydrothermal mound, Mid-Atlantic Ridge', *Phys. Earth Plan. Int., 109*, 201 - 212, 1998.

Kümpel, H.-J., Poroelasticity: parameters reviewed, *Geophysical Journal International, 105*, 783 - 799, 1991.

Le Prevost, C., Genco, M.L., Lyard, F., Vincent, P. and P. Canceil, Spectroscopy of the world ocean tides form a finite element hydrodynamic model, *J. Geophys. Res., 99*(C12), 24777 - 24797, 1994.

Le Prevost, C., Bennett, A.F. and D.E. Cartwright, Ocean tides for and from TOPEX/POSEIDON, *Science, 267*, 639 - 642, 1995.

Little, S.A., Stolzenbach, K.D. and F.J. Grassle, Tidal current effects on temperature in diffuse hydrothermal flow: Guaymas Basin, *Geophys. Res. Lett., 15*(13), 1491 - 1494, 1988.

Little, S.A., Stolzenbach, K.D. and F.J. Grassle, Correction to "Tidal current effects on temperature in diffuse hydrothermal flow: Guaymas Basin", *Geophys. Res. Lett., 16*(8), 985 - 986, 1989.

McDuff R.E. and J.R. Delaney, Periodic variability in fluid temperature at a seafloor hydrothermal vent, *Eos, Trans. AGU, Fall Meet. Suppl., 76*, p. 710, 1995.

Murphy W., Reischer, A. and K. Hsu, Modulus decomposition of compressional and shear velocities inn sand bodies, *Geophysics, 58*(2), 227 - 239, 1993.

Nur, A. and J.D. Byerlee, An exact effective stress law for elastic deformation of rock with fluids, *J. Geophys. Res., 76*(26), 6414 - 6419, 1971.

Phillips, O. M., *Flow and Reactions in Permeable Rocks*. Cambridge University Press, 1991.

Rice, J.R. and M.P. Cleary, Some basic stress diffusion solutions for fluid-saturated elastic porous media with compressible constituents, *Rev. Geophys. Space Phys., 14*(2), 227 - 241, 1976.

Rudnicki, M.D., James, R.H. and H. Elderfield, Near-field variability of the TAG non-buoyant plume, 26N, Mid-Atlantic Ridge, *Earth Plan. Sci. Lett., 127*, 1 - 10, 1994.

Sato, T., Kasahara, J. and K. Fujioka, Observation of pressure change associated with hydrothermal upwelling at a seamount in the south Mariana Trough using an ocean bottom seismometer, *Geophys. Res. Lett., 22*(11), 1325 - 1328, 1995.

Schrama, E.J.O. and R.D. Ray, A preliminary tidal analysis of TOPEX/POSEIDON altimetry, *J. Geophys. Res., 99*(C12), 24,799 - 24,808, 1994.

Schultz, A., Delaney, J.R. and R.E. McDuff, On the partitioning of heat flux between diffuse and point source seafloor venting, *J. Geophys. Res., 97*(B9), 12,299 - 12,314, 1992.

Schultz, A., Dickson, P. and H. Elderfield, Temporal variations in diffuse hydrothermal flow at TAG, *Geophys. Res. Lett., 23*(23), 3471 - 3474, 1996.

Sengers, J.V. and B. Kamgar-Parsi, Representative equations for the viscosity of water substance, *J. Phys. Chem. Ref. Data, 13*, 185 - 205, 1984.

Sengers, J.V. and J.T.R. Watson, Improved international formulation for the viscosity and thermal conductivity of water substance, *J. Phys. Chem. Ref. Data, 15*, 1291 - 1314, 1986.

Schwiderski, E.W., On charting global ocean tides, *Rev. Geophy. Space Phys., 18*(1), 243 - 268, 1980.

Tolstoy, M., Vernon, F.L., Orcutt, J.A. and Wyatt, F.K., Breathing of the seafloor: Tidal correlations of seismicity at Axial volcano *Geology, 30*(6), 503-506, 2002.

Turcotte, D.L. and G. Schubert, *Geodynamics: Applications of continuum physics to geological problems*, 450 pp., (John Wiley and Sons, New York), 1982.

Van der Kamp, G. and J.E. Gale, Theory of earth tide and barometric effects in porous formations with compressible grains, *Water Resour. Res., 19*(2), 538 - 544, 1983.

Van Wylen, G.J. and R.E. Sonntag, *Fundamentals of classical thermodynamics, SI version*, 2nd edition, 744 pp., (John Wiley and Sons, New York), 1978.

Wang, K. and E.E. Davis, Theory for the propagation of tidally induced pore pressure variations in layered subseafloor formations, *J. Geophys. Res., 101*(B5), 11483 - 11495, 1996.

Wang, K., van der Kamp, G. and E.E. Davis, Limits of tidal energy dissipation by fluid flow in subsea formations, *Geophys. J. Int., 139*, 763 - 768, 1999.

Watson, J.T.R., Basu, R.S. and J.V. Sengers, An improved representative equation for the dynamic viscosity of water substance, *J. Phys. Chem. Ref. Data, 9*, 1255 - 1290, 1980.

Wetzler, M.A., Lavelle, J.W., Cannon, G.A. and E.T. Baker, Variability of temperature and currents measured near Pipe Organ hydrothermal vent site, *Marine Geophys. Res., 20*(6), 505 - 516, 1998.

T. E. Jupp, BP Institute for Multiphase Flow, University of Cambridge, Madingley Rise, Madingley Road, Cambridge, CB3 0EZ, U.K. (e-mail: tim@bpi.cam.ac.uk)

A. Schultz, School of Earth Sciences, Cardiff University, Cardiff, CF10 3YE, U.K. (e-mail: adam@ocean.cf.ac.uk)

(Received _____.)